

Research Progress of Fiber-based Coherent Polarization Beam Combining for Free-Space Optical Communications in IOE, CAS

Yan Yang^{1,2,3}, Chao Geng^{1,2,*}, Xinyang Li^{1,2}, Feng Li^{1,2} and Guan Huang^{1,2,3}

¹*Institute of Optics and Electronics, Chinese Academy of Sciences, Chengdu, Sichuan 610209, China*

²*Key Laboratory on Adaptive Optics, Chinese Academy of Sciences, Chengdu, Sichuan 610209, China*

³*University of Chinese Academy of Sciences, Beijing 100049, China*

Keywords: Free-Space Optical Communications, Coherent Polarization Beam Combining, Fiber Optics.

Abstract: Multi-aperture receiver with phased array is an effective approach to overcome the atmospheric turbulence effect on the performance of the fiber-based free-space optical (FSO) communications, where how to combine the multiple beams received by the sub-apertures efficiently is one of the key techniques. In this paper, we report on the research progress of the fiber-based coherent polarization beam combining (CPBC) in IOE, CAS, which is a promising beam combining solution for coherent FSO communications employing the multi-aperture receiver. Phase-locking control and polarization-transforming control were proposed to combine linearly polarized beams with orthogonal polarizations into one linearly polarized beam efficiently, and three fiber-based CPBC schemes were proposed and experimentally validated.

1 INTRODUCTION

With the development of the Space-Ground Integration Network (SGIN), the demand of a higher link capacity is indubitable. Compared to the conventional radio frequency (RF) links, the free-space optical (FSO) communications offers numerous advantages including: ultra-high data rates, excellent security and large, unlicensed bandwidth, relatively low power consumption, and immunity to the electromagnetic interference (Chan, 2006). As the receiver sensitivity can be improved by up to 20 dB compared with that of non-coherent intensity modulation/ direct detection (IM/DD) scheme, the coherent FSO communications has great potential to be used in various applications (Agrawal, 2002). Currently, research has tended to focus on fiber-based coherent FSO communication systems, which can take advantage of the established components of fiber-optic communication systems (Li et al., 2016). In such schemes, efficiently coupling the signal light wavefront to optical fiber to achieve high received signal-to-noise ratio is critical (Zhang et al., 2013). The obvious means to increasing the received optical power is to increase the aperture diameter. However, optical telescopes with large apertures are very expensive and difficult to build. Furthermore, atmospheric turbulence adds to the difficulty of

coupling the signal light wavefront from large telescopes into optical fiber (Ma et al., 2015). To overcome the atmospheric turbulence effect, adaptive optics (AO) technology can be applied, and the receiver employing a monolithic aperture with AO has been demonstrated to be available to improve the coupling efficiency in fiber-based coherent FSO communications (Zheng et al., 2017). Nevertheless, when AO is used, equipment such as tip/tilt mirror (TM), deformable mirror (DM) and Hartmann Wavefront Sensor (WFS) is needed, which is complicated, costly and hard to achieve. As an alternative, the multi-aperture receiver with phased array (Yang et al., 2017) combines signals detected by sub-apertures to ease deep fades and increase the received optical power, in which adaptive fiber-optics coupler (AFOC) array (Li et al., 2017) is employed to correct the tip/tilt aberrations and promote the coupling efficiency of each sub-aperture. Compared with the receiver employing a monolithic aperture with AO, the multi-aperture receiver with phased array has easier manufacture, lower costs, superior reliability, smaller sub-aperture sizes, and more flexible sub-aperture positions (Yang et al., 2017). In the multi-aperture receiver with phased array, it is necessary to combine the signals from the aperture array, to merge these signals and enhance the received signal-to-noise

ratio.

In this paper, we report on the research progress of the fiber-based coherent polarization beam combining (CPBC) in IOE, CAS, which can be applied to combine multiple laser beams to one laser beam in the fiber-based coherent FSO communications employing multi-aperture receivers with phased array.

2 BASIC SCHEMES FOR FIBER-BASED CPBC

The fiber-based polarization beam combiner (PBC) (Yang et al., 2017), as shown in Figure 1, is the key device of the fiber-based CPBC, with the function of combining two orthogonally polarized fiber beams into one output fiber. Three polarization-maintaining fibers (PMFs) are fused in the two sides of the calcite prism. The slow axes of the PMFs in port-1 and port-2 are aligned to the Y axis and the X axis, respectively. The slow axis of the PMF in port-3 is rotated 45° clockwise by port-1.

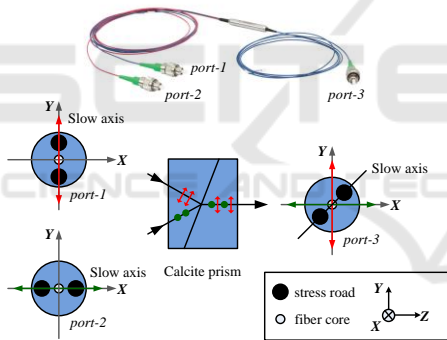


Figure 1: Structural schematic diagram of the fiber-based PBC.

The basic principle of the fiber-based CPBC is shown in Figure 2. It is well known that two linearly polarized beams with orthogonal polarizations can be combined into one beam by using a fiber-based PBC.

Theoretically, when the phase difference between the input beams is random, the polarization state of the combined beam is not a linearly polarized one, and it is just a superposition of the polarization states of the input beams, as shown in Figure 2(a).

Two methods can be employed to control the combined beam to be linearly polarized.

As shown in Figure 2(b), fiber-based CPBC with phase-locking (PL) control compensates for the

phase difference between the input beams by using the piezoelectric-ring fiber-optic phase compensators (PCs) to control the combined beam to be linearly polarized. Provided that the phase difference between the input beams is controlled to be $2n\pi$ (where n is an integer), the combined beam is linearly polarized, and the polarization direction is related on the power ratio of the input beams. Owing to that the slow axis of the PMF in port-3 is rotated 45° clockwise by port-1, the combined beam is linearly polarized along the slow axis of the PMF only when the power ratio of the input beams is equal to be 1. If the power ratio of the input beams is not equal to be 1, the polarization direction of the combined beam deviates from the slow axis of the PMF, which will significantly diminish the combining efficiency and limit the expansibility of the CPBC.

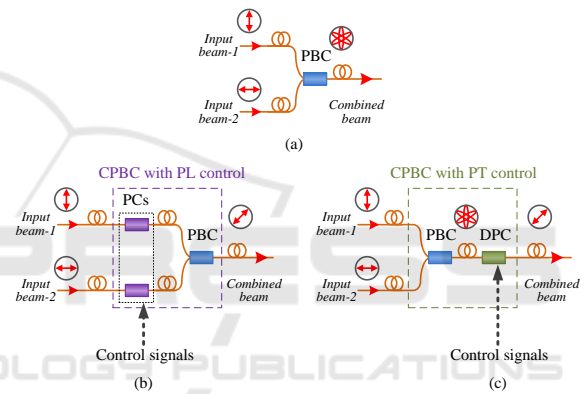


Figure 2: Basic principle of the fiber-based CPBC (a) without control, (b) with PL control, and (c) with PT control.

The combining efficiency η_{PL} is defined to be the ratio of the combined optical power along the slow axis of the PMF in port-3 and the total input optical powers. Without considering the excess loss of the fiber-based PBC, the relationship between the combining efficiency and the power ratio of the input beams I_R can be expressed by:

$$\eta_{PL} = \frac{1}{2} \times \frac{(1 + \sqrt{I_R})^2}{1 + I_R} \quad (1)$$

where the phase difference between the input beams is controlled to be $2n\pi$.

As shown in Figure 2(c), fiber-based CPBC with polarization-transforming (PT) control transforms the combined beam to be linearly polarized directly by using the dynamic polarization controller (DPC) (Yang et al., 2017), which can transform arbitrary polarization state to any desired polarization state.

When PT controlled, the combined beam can be linearly polarized along the slow axis of the PMF whether the input beams are phase-unlocked or beam-imbalanced.

The basic experimental setup of the fiber-based CPBC with two input beams is carried out, as shown in Figure 3. Two input beams are produced by splitting the output of a linearly polarized single-mode fiber laser at 1064 nm (NKT photonics). A variable optical attenuator (VOA), used for beam attenuating, is adopted in one of the input paths to adjust the power ratio of the input beams. Two input beams are combined by fiber-based CPBC. Then, the fiber-based polarization beam splitter (PBS), which has a similar structure to the fiber-based PBC except that the slow axis of the PMF in port-3' is identical to the slow axis of the PMF in port-1', with two photo detectors (PDs) is employed to stabilize the polarization state of the combined output beam and evaluate the performance of the combination. The PDs are PDA36A silicon amplifier detectors, produced by THORLABS Corporation. The optical power output from port-1', denoted as P_1' , is sent to a servo PD to provide a control signal as the cost function, and the stochastic parallel gradient descent (SPGD) algorithm (Geng et al., 2013) is employed to maximize the cost function. To quantitatively evaluate the CPBC performance, the optical power output from the port-2' is acquired by a detected PD, and denoted as P_2' . We use the coherent polarization combining efficiency (CPCE) η defined in Eq. (2) as a figure-of-merit:

$$\eta = \frac{P_1'}{P_1' + P_2'} \quad (2)$$

In the experimental setup, the fiber-based PBC is produced by Advanced Fiber Resources (AFR) Corporation, with the excess loss of no more than 0.8 dB at 1064 nm without connectors. The PC made by our group has a half-wave voltage of 1.3 V and a frequency response of about 32 kHz. The DPC is a kind of phase retardation-control polarization controller based on the principle of squeezing the fiber, with a response time of 30 μ s and the insertion loss of no more than 0.05 dB without connectors, produced by General Photonics.

First, the feasibilities of the two fiber-based CPBC schemes are validated by combining two input beams with identical optical powers.

The fiber-based CPBC with PL control is adopted in the setup, and the SPGD algorithm generates two PL control signals to control the PCs to compensate for the phase difference between the input beams. The iteration rate of the SPGD

algorithm is about 10 kHz, and the durations of the open and closed states are both 6 s. The experimental results are shown in Figure 4(a). The average CPCE increases from 74.18% in the open loop to 99.31% in the closed loop, and the mean square error (MSE) decreases from 0.3041 in the open loop to 0.0017 in the closed loop. The closed loop of PL control is achieved after about 25 iterations, equivalent to 2.5 ms, of SPGD optimization.

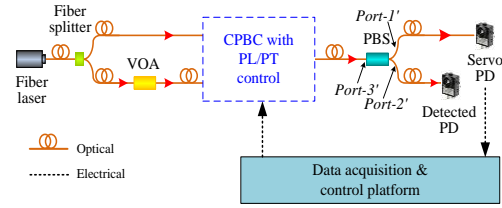


Figure 3: Experimental setup of the fiber-based CPBC with two input beams.

The fiber-based CPBC with PT control is adopted in the setup, and the SPGD algorithm generates four PT control signals to control the DPC to convert the polarization of the combined beam. The iteration rate of the SPGD algorithm is about 6 kHz, and the durations of the open and closed states are both 10 s. The experimental results are shown in Figure 4(b). The average CPCE increases from 62.03% in the open loop to 99.61% in the closed loop, and the MSE decreases from 0.0572 in the open loop to 0.0028 in the closed loop. The closed loop of PT control is achieved after about 20 iterations, equivalent to 3.3 ms, of SPGD optimization.

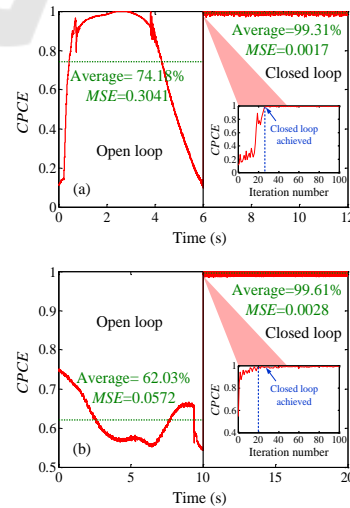


Figure 4: The experimental results of in fiber-based CPBC with (a) PL control and (b) PT control.

Then, we intentionally increase the difference between the optical powers of the two input beams to demonstrate the influence in the two fiber-based CPBC schemes. The results are shown in Figure 5. The blue curve represents the theoretical results of the CPBC with PL control calculated by using Eq. (1). The red curve and the green curve represent the experimental results of the CPBC with PL control and the CPBC with PT control, respectively, in which each point is averaged by ten experimental results with the specific power ratio. On the one hand, the experimental data in the fiber-based CPBC with PL control are reasonably consistent with the theoretical analysis, validating the conclusion that the power imbalance will significantly diminish the *CPCE* in the fiber-based CPBC with PL control. On the other hand, the *CPCE* is near constant at all power ratios with an average of 99.48% in the fiber-based CPBC with PT control, which indicates that the fiber-based CPBC with PT control can accommodate the power imbalance of the input beams and combine two input beams with arbitrary power ratio efficiently.

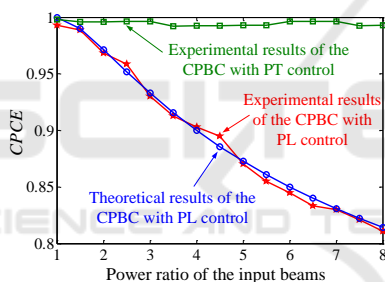


Figure 5: Curves of *CPCE* as the function of the power ratio of the input beams.

Both of the two fiber-based CPBC schemes have some limitations that will restrict the enhancement of the combining performance. In the fiber-based CPBC with PL control, the power imbalance of the input beams will inevitably degrade the combining efficiency of the CPBC and cannot be compensated. In the fiber-based CPBC with PT control, a major drawback is the increased complexity and decreased convergence rate due to the required multiple control signals.

3 IMPROVED SCHEME FOR FIBER-BASED CPBC

To break through the limitations in previous fiber-based CPBC schemes, the fiber-based CPBC with

cascaded PL and PT controls is proposed, as shown in Figure 6, to combine imbalanced laser beams (the number of the input beams is not binary). It is the synthesis of the PL control and PT control. When the input beams are balanced, PL control module is adopted; when the input beams are imbalanced, PT control module is employed. Moreover, the fiber-based CPBC with cascaded PL and PT controls can be scaled to combine multiple laser beams efficiently, and it can incorporate the advantages of the PL control and the PT control together. Compared with the CPBC based on PL control, in which the influence of the power imbalance on the combining performance is unavoidable, the proposed CPBC can combine imbalanced input beams with lower loss and higher combining efficiency. Compared with the CPBC based on PT control, the proposed CPBC needs less control signals, which will result in a lower complexity and faster convergence rate.

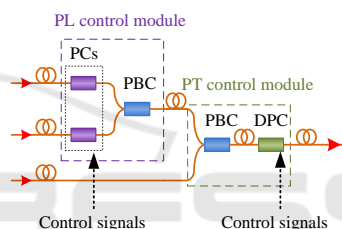


Figure 6: Basic principle of the fiber-based CPBC with cascaded PL and PT controls.

The basic experimental setup of fiber-based CPBC of three laser beams with cascaded PL and PT controls is carried out, as shown in Figure 7. Three input beams are produced by splitting the output of a linearly polarized single-mode fiber laser at 1064 nm, and three VOAs are employed in the input paths to adjust the optical powers of the input beams. The VOAs are not the essential parts of the CPBC setup and are used only for beam attenuating. Two of the three input beams with identical optical powers are firstly combined in a PL control module. To compensate for the phase difference between the two input beams and make the sub-combined beam to be linearly polarized, two PCs are employed in the input paths before fiber-based PBC-1 for PL control. With the loop closed, the PL control module produces a new, linearly polarized sub-combined beam, while the polarization direction is aligned to the slow axis of the PMF, as the two input beams are power balanced and phase locked. By transmitting in the PMF, the polarization state of the sub-combined beam remains unchanged. When incident at the fiber-based PBC-2 in the PT control module, the

polarization directions of the sub-combined beam and the third input beam are orthogonal. Thus, the two beams can be further coherently combined using the fiber-based PBC-2. To transform the combined beam to be linearly polarized, a DPC is employed after the fiber-based PBC-2 for PT control. The polarizer, with a PD is employed to stabilize the polarization state of the combined beam and evaluate the performance of the combination. In the setup, the SPGD algorithm is employed to perform the PL and PT controls. The optical power of the output beam acquired by the PD is chosen as the cost function. The control methods of the PL and PT controls are similar to each other except for the different values of the control coefficients δ and γ . The SPGD algorithm generates two PL control signals and four PT control signals simultaneously.

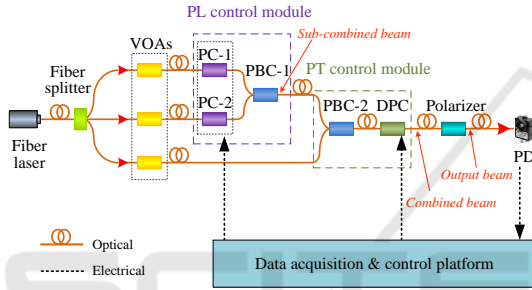


Figure 7: Basic experimental setup of the fiber-based CPBC of three laser beams with cascaded PL and PT controls.

In the experiment of the fiber-based CPBC with two input beams, the $CPCE$ defined in Eq. (2) is used to evaluate the performance of the combination. Nevertheless, it is inaccurate to evaluate the performance of the combination with more than two input beams. Considering all the device losses in the experimental setup, link budget can be derived out.

We assume that the optical powers of the three input beams are denoted as P_1 , P_2 , and P_3 , respectively.

The optical power of the sub-combined beam combined in the PL control module can be expressed by:

$$P_{\text{sub}} = (P_1 \times 10^{-IL_{PC-1}/10} + P_2 \times 10^{-IL_{PC-2}/10}) \times 10^{-EL_{PBC-1}/10} \times \eta_{PL} \quad (3)$$

where IL_{PC-1} is the insertion loss of the PC-1, IL_{PC-2} is the insertion loss of the PC-2, and EL_{PBC-1} is the excess loss of the fiber-based PBC-1. η_{PL} can be calculated by using Eq. (1), and here I_R is equal to be:

$$I_R = \frac{P_2}{P_1} \times 10^{(IL_{PC-1} - IL_{PC-2})/10} \quad (4)$$

The optical power of the combined beam combined in the PT control module can be expressed by:

$$P_{\text{com}} = (P_{\text{sub}} + P_3) \times 10^{-EL_{PBC-2}/10 - IL_{DPC}/10} \quad (5)$$

where IL_{DPC} is the insertion loss of the DPC, and EL_{PBC-2} is the excess loss of the fiber-based PBC-2.

The optical power of the output beam can be expressed by:

$$P_{\text{out}} = P_{\text{com}} \times 10^{-IL_P/10} \quad (6)$$

where IL_P is the insertion loss of the polarizer.

In the experiment, the optical powers of the three input beams are equal to be 0.55 mW, 0.55 mW, and 0.2 mW, respectively. The efficiency losses of the fiber devices employed in the experiment are measured as follows: $IL_{PC-1}=0.45$ dB, $IL_{PC-2}=0.45$ dB, $EL_{PBC-1}=0.93$ dB, $EL_{PBC-2}=0.81$ dB, $IL_{DPC}=0.55$ dB, $IL_P=0.63$ dB. By using Eq. (3), Eq. (4), Eq. (5), and Eq. (6), it can be calculated that after combination, the theoretical optical power of the output beam is 0.63 mW. In fact, the combined optical power can be further enhanced by fiber fusion technique to reduce the losses caused by the connectors.

To evaluate the CPBC performance, we use the combining efficiency η' defined in Eq. (7) as a figure of merit:

$$\eta' = \frac{P_{\text{det}}}{P_{\text{out}}} \times 100\% \quad (7)$$

where P_{det} is the detected optical power of the output beam in the experiment.

The experimental results are shown in Figure 8. The iteration rate of the SPGD algorithm is about 6 kHz. The durations of the open and closed states are both 10 s. The average combining efficiency increases from 18.23% in the open loop to 95.81% in the closed loop, and the MSE decreases from 0.1475 in the open loop to 0.0044 in the closed loop. The closed loop is achieved after about 20 iterations, equivalent to 3.3 ms, of SPGD optimization.

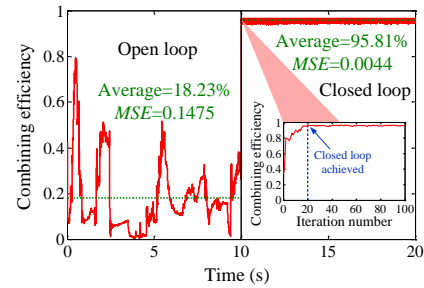


Figure 8: Experimental results of the fiber-based CPBC of three laser beams.

Supposing that the power imbalance of the input beams in the second-stage combination cannot be compensated, a small portion of the optical powers will be lost, and the optical power of the output beam can be expressed by:

$$P'_{\text{out}} = (P_{\text{sub}} + P_3) \times \left[\frac{1}{2} \times \frac{\left(1 + \sqrt{\frac{P_3}{P_{\text{sub}}}} \right)^2}{1 + \frac{P_3}{P_{\text{sub}}}} \right] \times 10^{-E_{\text{LDBC}}/10 - I_{\text{LDBC}}/10} \times 10^{-I_{\text{L}}/10} \quad (8)$$

After calculation, it can be noted that P'_{out} is equal to be 0.57 mW.

The average optical power of the output beam detected in the experiment is 0.60 mW when loop closed, and greater than the theoretical optical power of the output beam under the assumption that the power imbalance of the input beams in the second-stage combination cannot be compensated, which indicates that the fiber-based CPBC with cascaded PL and PT controls can break through the limitation in the fiber-based CPBC with PL control that the power imbalance will restrict the combining efficiency, and can combine three laser beams to one linearly polarized beam efficiently.

On the other hand, in the fiber-based CPBC of three beams with PT control, two DPCs as well as eight control signals are required. It is obvious that the closed loop will be achieved after more than 3.3 ms (the experimental results of fiber-based CPBC of two input beams) of SPGD optimization in the experiment of fiber-based CPBC of three laser beams with PT control. It can be noted that, compared with the fiber-based CPBC with PT control, the fiber-based CPBC with cascaded PL and PT controls needs less control signals, resulting in a lower complexity and faster convergence rate.

4 CONCLUSION

In conclusion, we have reported on the research progress of the fiber-based CPBC in IOE, CAS. Two control strategies, PL control and PT control, are proposed and experimentally validated. It can be noted that the CPBC with PL control and CPBC with PT control both can combine individual beams efficiently. Nevertheless, both of the two fiber-based CPBC schemes have some limitations that will restrict the enhancement of the combining performance. In the CPBC with PL control, the power imbalance of the input beams will inevitably degrade the combining efficiency of the CPBC and

cannot be compensated. In the CPBC with PT control, a major drawback is the increased complexity and decreased convergence rate due to the required multiple control signals. To break through the limitations in previous fiber-based CPBC schemes, the CPBC with cascaded PL and PT controls is proposed. It is the synthesis of the PL control and PT control, and can combine the advantages of the PL control and the PT control together. We believe that the proposed fiber-based CPBC in this paper has great potential in coherent FSO communications employing the multi-aperture receiver with phased array.

This work is supported by the National Natural Science Foundation of China under grant No. 61675205 and the CAS "Light of West China" program.

REFERENCES

- Chan, V. W. S., 2006. Free-space optical communications. *J. Lightwave Technol.* 24/12, 4750–4762.
- Agrawal, G. P., 2002. Fiber-Optic Communication Systems. A John Wiley & Sons, Inc. 3rd edition.
- Li, K., Ma, J., Tan, L., Yu, S., Zhai, C., 2016. Performance analysis of fiber-based free-space optical communications with coherent detection spatial diversity. *Appl. Opt.* 55/17, 4649–4656.
- Zhang, R., Wang, J., Zhao, G., Lv, J., 2013. Fiber-based free-space optical coherent receiver with vibration compensation mechanism. *Opt. Express* 21/15, 18434–18441.
- Ma, J., Ma, L., Yang, Q., Ran, Q., 2015. Statistical model of the efficiency for spatial light coupling into a single-mode fiber in the presence of atmospheric turbulence. *Appl. Opt.* 54/31, 9287–9293.
- Zheng, D., Li, Y., Li, B., Li, W., Chen, E., Wu, J., 2017. Free space to few-mode fiber coupling efficiency improvement with adaptive optics under atmospheric turbulence. 2017 *Optical Fiber Communications Conference and Exhibition (OFC)*.
- Yang, Y., Geng, C., Li, F., Huang, G., Li, X., 2017. Multi-aperture all-fiber active coherent beam combining for free-space optical communication receivers. *Opt. Express* 25/22, 27519–27532.
- Li, F., Geng, C., Huang, G., Yang, Y., Li, X., Qui, Q., 2017. Experimental demonstration of coherent combining with tip/tilt control based on adaptive space-to-fiber laser beam coupling. *IEEE Photon. J.* 9/2, 7102812.
- Yang, Y., Geng, C., Li, F., Li, X., 2017. Combining module based on coherent polarization beam combining. *Appl. Opt.* 56/7, 2020–2028.
- Yang, Y., Geng, C., Li, F., Huang, G., Li, X., 2017. Coherent polarization beam combining approach based on polarization controlling in fiber devices. *IEEE Photon. Technol. Lett.* 29/12, 945–948.

Geng, C., Luo, W., Tan, Y., Liu, H., Mu, J., Li, X., 2013. Experimental demonstration of using divergence cost-function in SPGD algorithm for coherent beam combining with tip-tilt control. *Opt. Express* 21/21, 25045–25055.

